Fabrication of phase-change $Ge_2Sb_2Te_5$ nano-rings

Cheng Hung Chu,[1,2] Ming Lun Tseng,[1] Chiun Da Shiue,[1] Shuan Wei Chen,[1] Hai-Pang Chiang,[2] Masud Mansuripur,[3] and Din Ping Tsai[1,4,5,*]

[1]Department of Physics, National Taiwan University, Taipei 106, Taiwan
[2]Institute of Optoelectronic Sciences, National Taiwan Ocean University, Keelung 202, Taiwan
[3]College of Optical Sciences, The University of Arizona, Tucson, Arizona 85721, USA
[4]Research Center for Applied Sciences, Academia Sinica, Taipei 115, Taiwan
[5]Instrument Technology Research Center, National Applied Research Laboratories, Hsinchu 300, Taiwan
**dptsai@phys.ntu.edu.tw*

Abstract: Phase-change material $Ge_2Sb_2T_5$ rings with nanometer-scale thickness have been fabricated using the photo-thermal effect of a focused laser beam followed by differential chemical etching. Laser irradiation conditions and etching process parameters are varied to control the geometric characteristics of the rings. We demonstrate the possibility of arranging the rings in specific geometric patterns, and also their release from the original substrate.

OCIS codes: (210.4810) Optical storage-recording materials; (310.3840) Materials and process characterization; (220.0220) Optical design and fabrication.

References and links

1. S. R. Ovshinsky, "Reversible electrical switching phenomena in disordered structures," Phys. Rev. Lett. **21**(20), 1450–1453 (1968).
2. N. Yamada, E. Ohno, K. Nishiuchi, N. Akahira, and M. Takao, "Rapid-phase transitions of GeTe-Sb_2Te_3 pseudobinary amorphous thin films for an optical disk memory," J. Appl. Phys. **69**(5), 2849–2856 (1991).
3. T. Ohta, K. Nagata, I. Satoh, and R. Imanaka, "Overwritable phase-change optical disk recording," IEEE Trans. Magn. **34**(2), 426–431 (1998).
4. T. Ohta, K. Nishiuchi, K. Narumi, Y. Kitaoka, H. Ishibashi, N. Yamada, and T. Kozaki, "Overview and the future of phase-change optical disk technology," Jpn. J. Appl. Phys. **39**(Part 1, No. 2B), 770–774 (2000).
5. K. Nakayama, K. Kojima, Y. Imai, T. Kasai, S. Fukushima, A. Kitagawa, M. Kumeda, Y. Kakimoto, and M. Suzuki, "Nonvolatile memory based on phase change in Se-Sb-Te glass," Jpn. J. Appl. Phys. **42**(Part 1, No. 2A), 404–408 (2003).
6. A. L. Pirovano, A. L. Lacaita, A. Benvenuti, F. Pellizzer, and R. Bez, "Electronic switching in phase-change memories," IEEE Trans. Electron. Dev. **51**(3), 452–459 (2004).
7. W. Welnic and M. Wuttig, "Reversible switching in phase-change materials," Mater. Today **11**(6), 20–27 (2008).
8. S. K. Lin, I. C. Lin, and D. P. Tsai, "Characterization of nano recorded marks at different writing strategies on phase-change recording layer of optical disks," Opt. Express **14**(10), 4452–4458 (2006).
9. C. H. Chu, B. J. Wu, T. S. Kao, Y. H. Fu, H. P. Chiang, and D. P. Tsai, "Imaging of recording marks and their jitters with different writing strategy and terminal resistance of optical output," IEEE Trans. Magn. **45**(5), 2221–2223 (2009).
10. C. B. Peng, L. Cheng, and M. Mansuripur, "Experimental and theoretical investigations of laser-induced crystallization and amorphization in phase-change optical recording media," J. Appl. Phys. **82**(9), 4183–4191 (1997).
11. P. K. Khulbe, E. M. Wright, and M. Mansuripur, "Crystallization behavior of as-deposited, melt quenched, and primed amorphous states of $Ge_2Sb_{2.3}Te_5$ film," J. Appl. Phys. **88**(7), 3926–3933 (2000).
12. T. S. Kao, Y. H. Fu, H. W. Hsu, and D. P. Tsai, "Study of the optical response of phase-change recording layer with zinc oxide nanostructured thin film," J. Microsc. **229**(3), 561–566 (2008).
13. K. P. Chiu, K. F. Lai, and D. P. Tsai, "Application of surface polariton coupling between nano recording marks to optical data storage," Opt. Express **16**(18), 13885–13892 (2008).
14. S. K. Lin, P. L. Yang, I. C. Lin, H. W. Hsu, and D. P. Tsai, "Resolving nano scale recording bits on phase-change rewritable optical disk," Jpn. J. Appl. Phys. **45**(No. 2B), 1431–1434 (2006).
15. Y. Zhang, S. Raoux, D. Krebs, L. E. Krupp, T. Topuria, M. A. Caldwell, D. J. Milliron, A. Kellock, P. M. Rice, J. L. Jordan-Sweet, and H.-S. P. Wong, "Phase change nanodots patterning using a self-assembled polymer lithography and crystallization analysis," J. Appl. Phys. **104**(7), 074312 (2008).
16. K. Y. Yang, S. H. Hong, D. K. Kim, B. K. Cheong, and H. Lee, "Patterning of $Ge_2Sb_2Te_5$ phase change material using UV nano-imprint lithography," Microelectron. Eng. **84**(1), 21–24 (2007).
17. S. Raoux, C. T. Rettner, J. L. Jordan-Sweet, A. J. Kellock, T. Topuria, P. M. Rice, and D. C. Miller, "Direct

#145698 - $15.00 USD Received 11 Apr 2011; revised 13 May 2011; accepted 30 May 2011; published 15 Jun 2011

observation of amorphous to crystalline phase transitions in nanoparticle arrays of phase change materials," J. Appl. Phys. **102**(9), 094305 (2007).
18. H. Yoon, W. Jo, E. Lee, J. Lee, M. Kim, K. Lee, and Y. Khang, "Generation of phase-change Ge–Sb–Te nanoparticles by pulsed laser ablation," J. Non-Cryst. Solids **351**(43-45), 3430–3434 (2005).
19. S. M. Yoon, K. J. Choi, Y. S. Park, S. Y. Lee, N. Y. Lee, and B. G. Yu, "Fabrication and electrical characterization of phase-change memory devices with nanoscale self-heating-channel structures," Microelectron. Eng. **85**(12), 2334–2337 (2008).
20. C. H. Chu, C. Da Shiue, H. W. Cheng, M. L. Tseng, H.-P. Chiang, M. Mansuripur, and D. P. Tsai, "Laser-induced phase transitions of $Ge_2Sb_2Te_5$ thin films used in optical and electronic data storage and in thermal lithography," Opt. Express **18**(17), 18383–18393 (2010).

1. Introduction

In the last few decades, several researches have been devoted to chalcogenide-based phase-change materials to explore the diverse optical and electrical properties of the easily-accessible phase states of these materials [1–14]. The phase-change material $Ge_2Sb_2T_5$ (GST) has been utilized as the recording medium in optical and electronic rewritable data storage because of its thermal stability and rapid transition between amorphous and crystalline states. Several efforts have focused on the patterning of this phase-change material. For example, self-assembled copolymer lithography and nano-imprint lithography together with etching techniques have been used to fabricate phase-change nano-dot arrays for phase-change memory [15,16]. Electron beam lithography and pulsed-laser ablation have been used to fabricate phase-change nano-particles [17,18]. Also, a dry etching method for the fabrication of nanoscale GST patterns using high-density helicon plasma etching system is proposed [19]. In our recent research, we have studied the formation of laser-assisted geometric patterns on as-deposited GST films using a static tester, and related the phase distributions of the resulting patterns to the illumination conditions [20]. In this paper we propose a lithographic technique consisting of laser-irradiation and selective wet etching for the fabrication of GST nano-rings. We have realized complex and movable GST structures (including a chain of nano-rings) by adjusting the laser irradiation conditions.

2. Experimental

Thin film stacks with the structure of ZnS-SiO_2 (130 nm)/$Ge_2Sb_2Te_5$ (50 nm), coated onto a glass substrate, were fabricated in a conventional magnetron sputtering machine (Shibaura). Samples with crystalline-state GST were obtained by annealing in an oven at 300°C for 15 minutes. Localized laser irradiation of the GST film was carried out in an optical pump-probe system (Static Media Tester, TOPTICA Co., Munich, Germany) with a red laser (wavelength = 658nm) focused through a 0.65NA objective lens. After laser irradiation, the samples were chemically etched in a 1 wt% concentration NaOH solution under magnetic stirring (550 rpm) for 40 minutes. The NaOH solution is known to have different etching rates for crystalline and amorphous states of GST. Characterization of surface morphology and pattern structure were carried out using an atomic force microscope (AFM, Asylum Research, Santa Barbara, USA). Optical microscopy was used for direct observation of the samples.

3. Result and discussion

Figure 1 shows AFM images of laser-fabricated grid patterns with a pulse duration of 700 ns and various incident laser powers (from 7 mW to 20 mW) on a 50nm-thick crystalline GST film before and after etching. The spacing between adjacent rings is 5 μm. In the case of the lowest applied power of 7 mW, nano-bumps are seen to have formed on the GST film, having a diameter of ~800 nm and a height of ~8 nm. Laser irradiation induces melting and mass-redistribution of the GST, concentrating the molten material at the center of the irradiated region. When the applied laser power is greater than 8 mW, well-defined circular ring patterns are obtained, with a ring-diameter that increases with the irradiation power; each pattern in this case consists of an ablated hole surrounded by a raised ring. Evaporation and thermal compression of the molten GST are responsible for the formation of the hole and the ring, respectively, the effects being enhanced by an increasing laser power.

#145698 - $15.00 USD Received 11 Apr 2011; revised 13 May 2011; accepted 30 May 2011; published 15 Jun 2011

We have shown in our previous work [20] that the NaOH etch-rate for the crystalline state of GST is greater than that for its amorphous state, so that the various phase states of the laser-recorded regions can be inferred from the patterns that survive the etching process. After 40 minutes of NaOH etching, the amorphous nano-bumps recorded with a laser power of 7 mW (and also the amorphous nano-rings recorded with a laser power of 8 mW) stay in place, but some of the raised amorphous rings recorded at higher laser powers separate from their crystalline host. This result indicates the formation of a "crystalline fracture region" between the rings and their surrounding material, with the etching process eroding the outer boundaries of the amorphous rings.

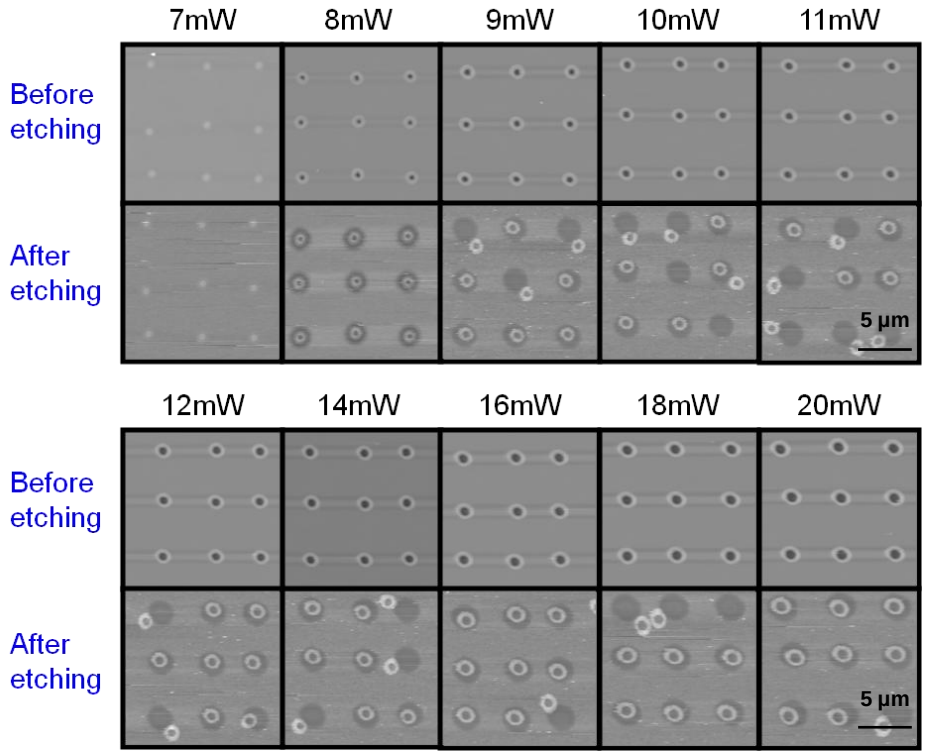

Fig. 1. AFM images of various ring structures before etching (top row) and after etching (bottom row) recorded on a crystalline $Ge_2Sb_2Te_5$ thin film with a focused laser beam having a pulse duration of 700ns at laser powers ranging from 7mW to 20mW.

Figure 2 shows the measured geometric characteristics of the fabricated patterns as functions of the applied laser power; each ring's characteristics before and after etching are shown in blue and red, respectively. The diameters of the rings, as measured by AFM, show the smallest width being 390 nm before etching and 370 nm afterward. The inner radius of the ring (i.e., the laser ablation hole) is ~200 nm at 8 mW laser power. A correlation between the ring size and laser power is observed in both Figs. 1 and 2; when the applied laser power increases, the absorption of thermal energy ablates more material. The height in Fig. 2(d) is defined as the distance between the top of the ring and the background. The heights are seen to increase after etching, approaching the thickness of the GST film (50 nm). Because the crystalline regions surrounding the rings are etched away, the complete appearance of amorphous rings is revealed. In the case of 8 mW laser power, the height difference before and after etching is less than the film thickness; this is due to the fact that the available thermal energy is insufficient to melt and then re-crystallize the entire thickness of the GST layer.

#145698 - $15.00 USD Received 11 Apr 2011; revised 13 May 2011; accepted 30 May 2011; published 15 Jun 2011

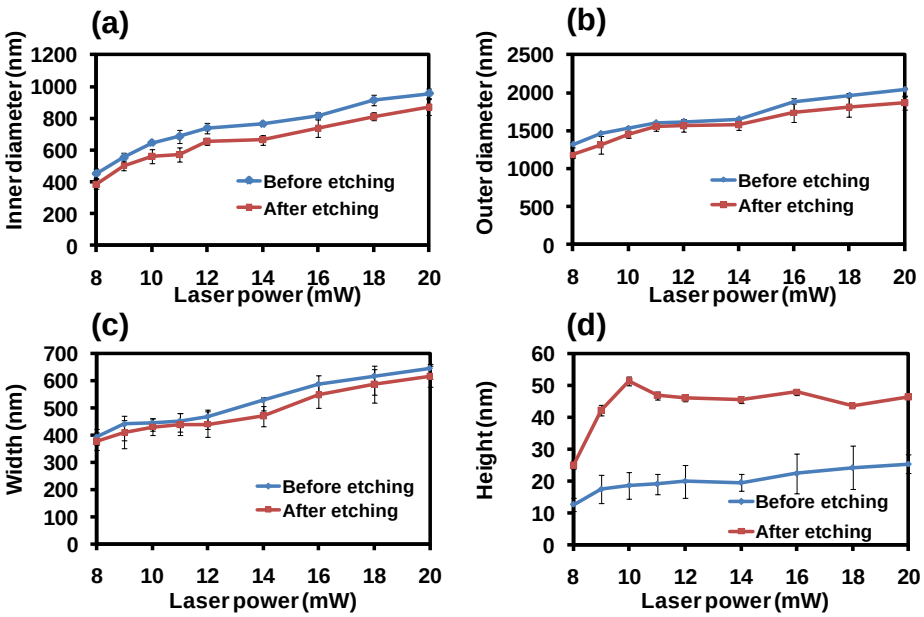

Fig. 2. Incident laser power dependence of (a) inner diameter, (b) outer diameter, (c) width, and (d) height of the rings before and after etching.

The topographic and optical images of the ring patterns recorded with a laser power of 16 mW and pulse duration of 700 ns on a crystalline GST film are shown in Fig. 3. Figures 3(a)–3(c) are, respectively, the AFM image, the optical reflection image, and the optical transmission microscopic image, all of them observed before etching. Figures 3(d)–3(f) show the corresponding images of the same region of the sample after 40 minutes of etching. The average outer diameter, inner diameter, and height are measured at 1.7 μm, 0.76 μm, and 48 nm, respectively. The remaining bright (raised) rings shown in the AFM image are believed to be GST in its amorphous state. From the reflection optical image of Fig. 3(b), we find the rings to be nearly as bright as the crystalline background, but the AFM image of the etched sample shows the rings to be in the amorphous state. The re-crystallized GST boundary between crystalline background and the amorphous ring is observed and identified after etching. This observation is in good agreement with the results obtained in our previous study, which included transmission electron microscopy (TEM) combined with local electron diffraction analysis [20]. For the etched sample, the mobile rings display high reflectivity and low transmissivity in the optical images. This may be caused by local crystalline GST grains embedded in the generally amorphous-state ring. Accordingly, it might be possible to control the optical properties of the rings by delivering different doses of laser energy.

#145698 - $15.00 USD Received 11 Apr 2011; revised 13 May 2011; accepted 30 May 2011; published 15 Jun 2011

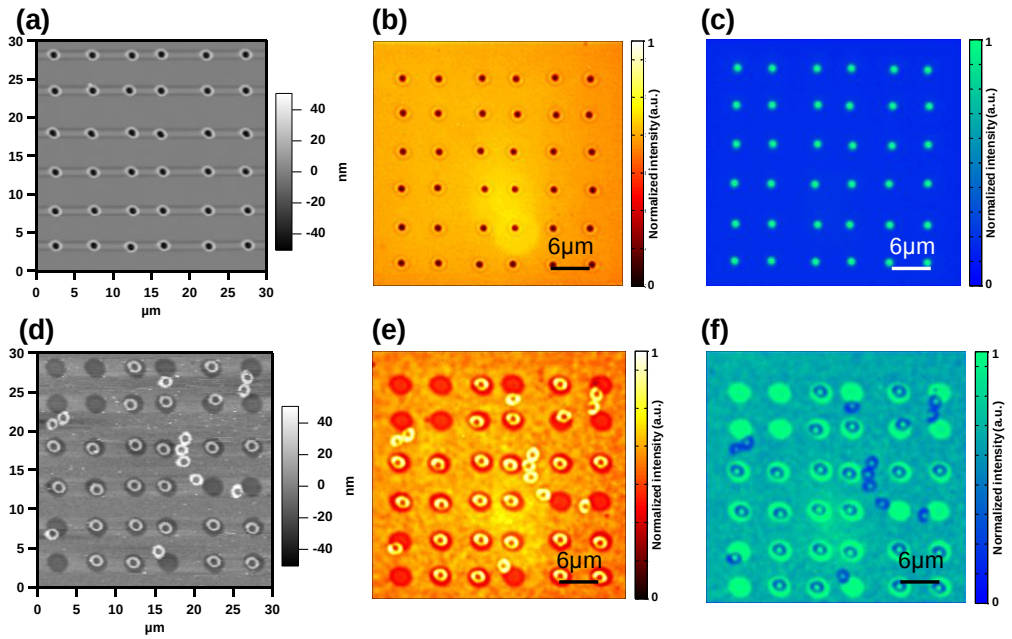

Fig. 3. AFM and optical images of rings recorded with a laser power of 16 mW and pulse duration of 700 ns on a crystalline $Ge_2Sb_2Te_5$ thin film. (a)-(c) AFM image, optical reflection image, and optical transmission image of the sample before etching. (d)-(f) AFM image, optical reflection image, and optical transmission image of the same region of the sample after 40 minutes of etching.

Two typical examples of the fabrication of specific patterns of rings appear in Fig. 4. Figures 4(a) and 4(b) show AFM images and cross-sectional profiles of a string of 5 rings and an Olympic symbol, recorded with the laser power of 16 mW and pulse duration of 700 ns on a 50nm-thick crystalline GST film. The outer diameter of each ring is 1.5 μm, and the height of the pattern is about 80 nm. The center-to-center spacing between adjacent rings is 2 μm, and experimental results confirm that the rings are overlapped and well-connected. Figures 4(c) and 4(d) are the corresponding AFM images (and cross-sectional profiles) of the same samples after etching in a 1.0 wt% NaOH solution for 40 minutes. The patterns are seen to have separated from their crystalline background. These AFM profiles also show the heights of the etched patterns to have decreased from 80 nm to about 45 nm.

4. Conclusion

The photo-thermal effect of a focused laser beam on a thin film of phase-change GST material generates crystalline and amorphous states, and the subsequent differential chemical etching removes crystalline material faster than the amorphous GST to produce movable rings. The diameter and thickness of the GST rings can be controlled by adjusting the irradiation conditions. GST rings with thickness of 25 nm to 48 nm, inner diameter of 390 nm to 760 nm, and ring width of 370 nm to 470 nm have been fabricated. Specific patterns such as a string of 5 rings and the Olympic symbol have been experimentally demonstrated, showing potential applications for phase-change GST-based opto-electronic devices.

#145698 - $15.00 USD Received 11 Apr 2011; revised 13 May 2011; accepted 30 May 2011; published 15 Jun 2011

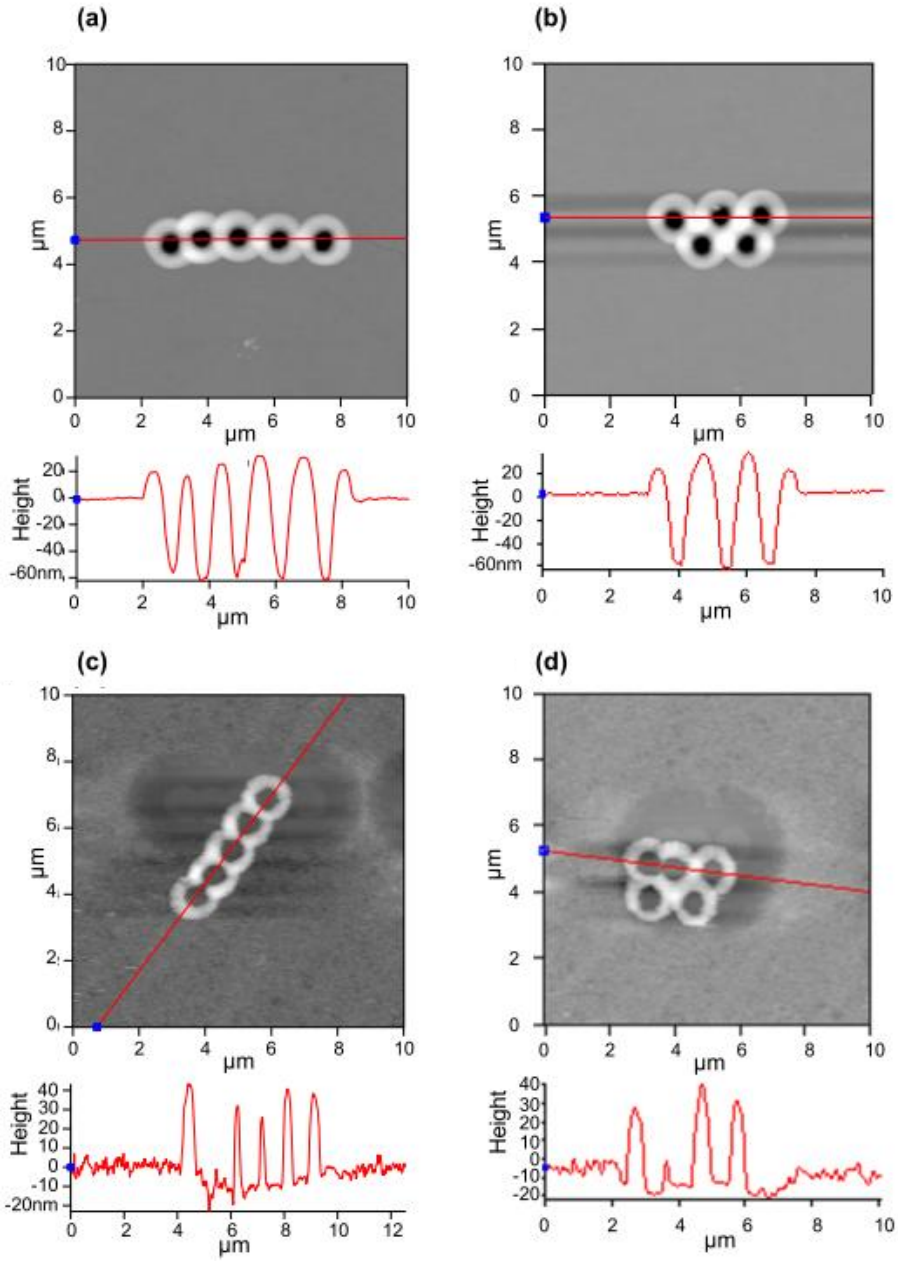

Fig. 4. AFM images of strings of 5 rings and the Olympic symbol fabricated by multiple laser pulses on a crystalline $Ge_2Sb_2Te_5$ thin film. The laser power and pulse duration were 16 mW and 700 ns for recording the pre-etch patterns shown in (a) and (b). AFM images of the etched samples are shown in (c) and (d). The corresponding cross-sectional profiles are also shown under individual AFM images.

Acknowledgments

The authors acknowledge financial support from National Science Council, Taiwan under grant numbers 99-2811-M-002-003, 99-2911-I-002-127, 99-2120-M-002-012 and 98-EC-17-A-09-S1-019.

#145698 - $15.00 USD Received 11 Apr 2011; revised 13 May 2011; accepted 30 May 2011; published 15 Jun 2011